Scientia Et Technica
ISSN: 0122-1701
scientia@utp.edu.co
Universidad Tecnológica de Pereira
Colombia

Peñafiel Guzmán, Evelyn; Bermúdez Turizo., Osmar; Duarte Forero, Jorge
CFD optimization of a heat exchanger for energy recovery in a stationary single-cylinder diesel engine
Scientia Et Technica, vol. 26, núm. 3, 2021, Agosto-Octubre, pp. 298-307
Universidad Tecnológica de Pereira
Pereira, Colombia

DOI: https://doi.org/10.22517/23447214.24557

Disponible en: https://www.redalyc.org/articulo.oa?id=84969623005

CFD optimization of a heat exchanger for energy recovery in a stationary single-cylinder diesel engine

Optimización CFD de un intercambiador de calor para la recuperación energética en un motor diésel monocilíndrico estacionario

E. Peñafiel-Guzmán ; O. Bermúdez-Turizo ; J. E. Duarte-Forero

DOI: https://doi.org/10.22517/23447214.24557
Artículo de investigación científica y tecnológica

***Abstract*— The implementation of thermoelectric generators (TEG) has been a promising response to the energy problem in internal combustion engines, which has motivated the study of the potential for energy recovery in the exhaust gas stream of a single-cylinder diesel engine using a thermoelectric generator, analyzing the importance of the heat exchanger geometry in the performance of the TEG. Considering many investigations, three different heat exchanger geometries were developed; the behavior of the exhaust gases was simulated with the OpenFOAM ® software, using a realizable $k-\varepsilon$ model, where a good quality mesh was established. In addition, a mesh independence study was performed, where stability was achieved from 1'000,000 elements. Experimental validation was carried out, and an average relative error of 2.23% was obtained, with which the results were classified as reliable. The simulations allowed the analysis of variables such as heat transfer, voltage, and current generated by thermoelectric modules, pressure drop, turbulence kinetic energy (TKE), and turbulence eddy dissipation rate (TEDR). Finally, it was obtained that the geometry with parallel paths had a better performance with respect to the analyzed variables, allowing a generation of 63.56 W, a pressure drop 92% lower than the other proposals, and better performance in the TKE and TEDR.**

***Index Terms*— Energy recovery, internal combustion engine, thermoelectric effect, thermoelectric generator.**

***Resumen*— La implementación de generadores termoeléctricos (TEG) ha sido una respuesta prometedora para la problemática energética en motores de combustión interna, lo cual ha motivado el estudio del potencial de recuperación energética en la corriente de gases de escape de un motor diésel monocilíndrico mediante un generador termoeléctrico, analizando la importancia de la geometría del intercambiador de calor en el desempeño del TEG. Tomando en cuenta diferentes investigaciones se desarrollaron tres geometrías diferentes de intercambiador de calor; el comportamiento de los gases de escape se simuló mediante el software OpenFOAM ® empleando un modelo $k-\varepsilon$ realizable, donde se estableció un mallado de buena calidad al que, además, se le realizó un estudio de independencia de malla en donde se alcanzó estabilidad a partir de 1'000.000 de elementos. Se hizo una validación experimental, con la que se obtuvo un error relativo promedio de 2.23%, con lo cual se calificaron los resultados como confiables. Las simulaciones permitieron el análisis de variables como la transferencia de calor, el voltaje y la corriente generado por los módulos termoeléctricos, la caída de presión, la energía cinética de turbulencia (TKE) y la tasa de disipación de la turbulencia (TEDR). Finalmente se obtuvo que la geometría con caminos paralelos tuvo un mejor desempeño con respecto a las variables analizadas, permitiendo una generación de 63.56 W, una caída de presión 92% menor a las otras propuestas, y un mejor desempeño en la TKE y TEDR.**

***Palabras claves*— Efecto termoeléctrico, generador termoeléctrico, motor de combustión interna, recuperación energética.**

I. Introduction

SINCE its creation in the 19th century, the Internal Combustion Engine (ICE) has helped to make life easier for human beings. Their great utility for passengers, food, and machinery transport, the multiple uses they have, the great power they generate, and the great autonomy of operation that

This manuscript was sent on October 28, 2020 and accepted on June 30, 2021. This work was supported in part by the Universidad del Atlántico through the project ING81-CII2019 "Estudio experimental de la sustitución parcial de combustible con HIDROXY (HHO) en motores térmicos de encendido por compresión y la influencia sobre sus prestaciones".

Osmar Bermúdez Turizo is with Universidad del Atlántico. Mechanical Engineering Program. Puerto Colombia, Colombia (e-mail: oabermudez@est.uniatlantico.edu.co).

Evelyn Peñafiel Guzmán is with Universidad del Atlántico. Mechanical Engineering Program. Puerto Colombia, Colombia (e-mail: epenafiel@est.uniatlantico.edu.co).

Jorge Duarte Forero is with Universidad del Atlántico. Mechanical Engineering Program. Puerto Colombia, Colombia (e-mail: jorgeduarte@mail.uniatlantico.edu.co).

their employment means have been their main attractive. Only in Europe, more than 50% of freight transport is carried out by the road, using vehicles that mostly operate with ICEs [1]. Nowadays, these types of engines have several applications in the field of mechatronics [2], becoming the central motivation of extensive studies; however, since their invention, ICEs feature a few disadvantages that have not been mitigated. For instance, it is found that only 12-25% of the energy produced by combustion is converted into useful work, while 30-40% of this energy is transformed to heat and then dissipated into the environment through the exhaust gases [3]. In addition, the transportation sector contributes by around 22% of global emissions of gases such as CO_2, CO, CH_4, NOx, etc., which affects climate change, global warming, and other environmental concerns [4]. Another important factor to consider is that ICEs depend approximately 94% on fossil fuels, which are non-renewable resources that are getting closer to their depletion, and as a consequence, prices are increasing [5]. To alleviate these harmful effects, different investigations have proposed several solutions for the operation of engines. For example, the new trend of fuels fosters environmentally friendly mixtures such as hydrogen-enriched biogas[6]. Others have proposed the possibility of creating hybrid vehicles [7] or transforming vehicles with combustion engines into electric vehicles [8] while reducing operating costs.

On the other hand, as a solution to the energy wasted in ICEs, different methods have been proposed. Some of them take advantage of the kinetic energy of the fluids in motion. An example is the use of turbo compounding on turbocharged diesel engines, which is an alternative highly studied in the field of energy recovery. However, this alternative has disadvantages in terms of reliability and high cost. Thereby, the weight that the system adds to the original engine configuration and space it occupies. In addition, when engines operate at low loads, there may be a little or negative gain of the turbocharging system [9].

Other alternatives for energy recovery include the utilization of exhaust gases from ICEs as the thermal source for power cycles. Organic Rankine Cycle (ORC) stands as one of the most suitable technologies for low-medium temperature sources. In fact, this cycle offers the most efficient performance for low-temperature thermal sources, such as most engine exhaust. Different configurations of the ORC cycle have been addressed, whereas the nature of the working fluid plays an important role within the optimal operation. Hoan and Hossain [10], [11] analyzed different working fluids to define the circumstances where certain fluid was most-suitable for energy recovery. However, the implementation of ORC technologies possesses a few disadvantages in terms of adaptability. Considering that a complete layout is designed for specific working conditions, namely pressure ratios and operational temperature; thus, any variation on the operation requires major modifications that boost investment costs. Moreover, energy production can be limited since some organic fluids have high density, which reduces turbine power output [12].

Among other techniques that employ thermal energy for energy recovery, Exhaust Gas Recirculation (EGR) is also found, whose main objective is to reduce NOx emissions. This method consists of forwarding a part of the exhaust gases to the intake manifold, causing a decrease in the oxygen content and combustion temperature so that the amount of NOx generated gets significantly reduced [13], [14]. The main disadvantage of EGR is that it increases the production of particles due to the low concentration of oxygen, and in certain cases, the engine can operate in areas with instabilities leading to power loss conditions [15].

In addition to the proposed solutions, Thermoelectric Generator (TEG) stands as a promising technology to produce electricity based on the Seebeck effect, which indicates that an electromotive force can be generated by temperature gradients. A TEG is composed of Thermoelectric Modules (TEM) or cells, which are located between a heat source and a heat sink; these generally comprise many pairs of thermoelectric couples, and each couple incorporates a pair of p- and n-type elements. These devices offer multiple advantages, such as zero emissions, compact volume, long service life, clean energy production, reduced noise, low maintenance cost, and high reliability [16]. Champier [17] demonstrated that the applications of TEGs are varied. They can be used for electricity generation in extreme environments, microgeneration with sensors and microelectronics, and in solar applications; especially, the robust operation is found for Waste Heat Recovery (WHR) applications, which is the main interest of the present study.

Temizer *et al.* [18] studied the performance of a TEG system in diesel engines using 40 thermoelectric modules, achieving a maximum power generation of 156.7 W. Vale *et al.* [19] recommend the implementation of TEGs for WHR applications on diesel vehicles that are used specifically in freight transport, since they travel long distances with high loads, producing exhaust gases at high temperatures on more stable roads than those of urban vehicle transportation. However, Fernandez-Yañez *et al.* [20] studied the potential of these devices in light-duty diesel engines, and although several challenges were faced, a modest amount of 24.2W was recovered. Mohamed [21] carried out the same study in a light diesel vehicle and reached a system efficiency of 4.63% under the European driving cycle conditions.

To improve energy recovery, Orr *et al.* [22] have studied the possibility of using TEGs and heat pipes, managing to reduce thermal resistance and pressure losses. However, as stated by Su *et al.* [23], the factors that foster efficient operation of the TEG are the thermal capacity and the heat transfer rate of the heat exchanger. Therefore, the continuous improvement of the last characteristics will result in more uniform temperature distribution and higher interface temperature producing higher power generation. To achieve this improvement in the design of different heat exchangers, Bhutta *et al.* [24] proposed using CFD (Computational Fluid Dynamics) simulations, which are tools that use numerical analysis and data structures to solve problems and analyze complex problems of flow interactions. In the same way, Chen *et al.* [25] used CFD tools to compare the behavior of different TEG configurations. They set a configuration with a single TEM and a configuration with two TEMs in tandem to figure out their performance. The comparative assessment identified the most-suitable TEM arrangement that improves the efficiency and the output power by around 25.2% and 53.5%, respectively. The CFD approach demonstrated that integrating heat exchangers and TEGs promotes energy generation, exhibiting great potential for the present study.

Among CFD tools, OpenFOAM® is useful in obtaining theoretical predictions of the behavior of different fluids. However, the results that it shows are determined by the selected model, mesh type, the geometric patterns, among other factors that influence the mesh independence analysis, which establishes the number of minimum elements that guarantee convergence and stability in the results. Among the variety of turbulence models for CFD simulations, the convectional $k-\varepsilon$ model features great performance to analyze the flow interactions. This model was implemented in the investigation of Pavan Kumar *et al.* [26] to analyze the influence of heat transfer and pressure drop in micro-fin helically coiled tubes applications. In this study, the effect of the Reynolds number, fin number, coil diameter, Nusselt number, and pressure drop was analyzed. Wei Chen lin *et al.* [27] also used the convectional $k-\varepsilon$ model to investigate the thermal-hydraulic characteristics of helically coiled tube heat exchangers for high temperature gas reactors. The present study also incorporates the $k-\varepsilon$ model for the simulations computed in OpenFOAM® software, in order to achieve the optimization of a heat exchanger for energy recovery in diesel engines.

II. METHODOLOGY

Taking into account the literature review, three different configurations for the heat exchanger were developed to verify the influence on energy recovery. To determine an optimal geometry for the heat exchanger, CFD simulations were employed to reveal the overall behavior of the exhaust gases when flowing through the different geometry arrays. The methodology implemented is shown in Fig. 1.

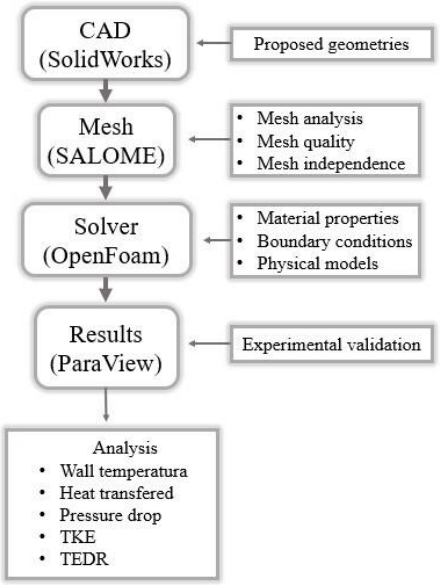

Fig. 1. Research Methodology

A. Computational fluid dynamics (CFD)

Computational fluid dynamics is a branch of fluid mechanics that uses numerical methods and other mathematical tools to solve fluid flow problems or simulate their behavior under specific conditions. Computational environments provide the calculations needed to simulate the interaction of fluids with projected surfaces. However, these calculations remain complex, and the results approximate physical phenomena to a greater or lesser extent depending on the complexity of the problem.

The basic structure of a CFD code is pre-processing, solving, and post-processing.

Solid and fluid domains are modeled, and the computational mesh is generated in the pre-processing section. SolidWorks and SALOME are the tools implemented in this stage of the CFD structure.

OpenFOAM® software works under the theory of finite volumes for fluids to obtain an approximated solution of the continuity, momentum, and energy equations. Thus, the application of the appropriate turbulence model reinforces the reliability of the solving stage of the CFD structure.

In the post-processing stage, the numerical and qualitative results generated by OpenFOAM® can be visualized using the complement Paraview.

The capacity of OpenFOAM® to predict the behavior of different variables and their influence on the energy recovery process makes it a useful tool to obtain an optimal geometry while minimizing costs of preliminary design as it is not necessary to manufacture all the geometries.

The selection of appropriate governing equations of the mathematical model is essential for an accurate prediction. For incompressible fluids, (1) and (2) are expressed as follows:

$$\frac{\partial U_j}{\partial x_j} = 0 \tag{1}$$

$$\frac{\partial U_i}{\partial t} + \frac{\partial U_i U_j}{\partial x_j} = -\frac{1}{\rho}\frac{\partial p}{\partial x_i} + \frac{\partial}{\partial x_j}\left[\frac{(\mu+\mu_t)}{\rho}\left(\frac{\partial U_i}{\partial x_j} + \frac{\partial U_j}{\partial x_i}\right)\right] \tag{2}$$

where the ρ is the fluid density, p is the pressure, U_i and U_j are the velocity components, μ is the laminar viscosity and μ_t is the turbulent viscosity [28].

For the turbulence model, the equations that describe turbulent the kinetic (k) and its dissipation rate (ε) interactions are described in (3) and (4):

$$\frac{\partial}{\partial t}(\rho k) + \frac{\partial}{\partial x_j}(\rho k u_j) = \frac{\partial}{\partial x_j}\left[\left(\mu + \frac{\mu_t}{\sigma_k}\right)\frac{\partial k}{\partial x_j}\right] + G_k + G_b - \rho\epsilon - Y_M + S_k \tag{3}$$

$$\frac{\partial}{\partial t}(\rho \epsilon) + \frac{\partial}{\partial x_j}(\rho \epsilon u_j) = \frac{\partial}{\partial x_j}\left[\left(\mu + \frac{\mu_t}{\sigma_\epsilon}\right)\frac{\partial \epsilon}{\partial x_j}\right] + \rho C_1 S_\epsilon - \rho C_2 \frac{\epsilon^2}{k+\sqrt{v\epsilon}} + C_{1\epsilon}\frac{\epsilon}{k}C_{3\epsilon}G_b + S_\epsilon \tag{4}$$

Here, G_k and G_b represent the generation of turbulence due to mean velocity gradients and buoyancy, respectively. Y_M is the contribution of the fluctuating dilatation in compressible turbulence to the overall dissipation rate. σ_k and σ_ϵ are the Prandtl number for k y ϵ, respectively. S_k y S_ϵ are the source terms for turbulence kinetic energy and turbulence dissipation rate [28]. The turbulence viscosity μ_t is expressed for (5):

$$\mu_t = \rho C_\mu \frac{k^2}{\epsilon} \tag{5}$$

The coefficients values of the convectional k – ε model are: $C_{1\epsilon} = 1.44$, $C_2 = 1.9$, $\sigma_k = 1.0$, $\sigma_\epsilon = 1.2$.

B. Influence of operational parameters on TEG performance

The proper operation of the thermoelectric devices in terms of power recovered is determined by the voltage and current generated, which, in turn, depends on the temperature difference between the hot and cold ends on each side of the modules, as shown in Fig. 2. Since the cooling system used for this generator is powered by water at room temperature (300.15 K), the greater the temperature of the exhaust gases, the greater the temperature difference. The heat transfer from the exhaust gases to the TEM can be increased through heat exchangers, so this study is mainly dedicated to promoting an optimal geometry that benefits not only the heat transfer but also most of the factors involved in the energy recovery process.

The pressure drops are another important variable involved in the process; indeed, high-pressure conditions compromise the operation of the engine on which the TEG is coupled. Notice that, within the initial conditions established for the simulations, it is assumed that the pressure at the outlet of the exchanger is 0 Pa gauge since this is what happens in reality. Therefore, the software iterates and performs the necessary calculations to determine the required pressure at the exhaust gases inlet so that the exchanger outlet pressure can be reached. If the pressure drop is minimal, it can be ensured that the exhaust gases reach the outlet pressure, and back pressure does not interfere with the performance of the engine.

The turbulence eddy dissipation rate (TEDR) and the turbulence kinetic energy (TKE) are decisive factors when selecting an optimal geometry for the heat exchanger. The first shows a parametrization of the mean dimension of eddies, which are desired to be small to reduce the iteration time of the non-linear turbulence equations [29]. The second is the average kinetic energy per unit mass associated with eddies generation in turbulent flows. This energy is produced by shear stress, friction, buoyancy, or external forces of the fluid at the scale of eddies, so it is always sought that the recirculation and vortex zones are minimal [29].

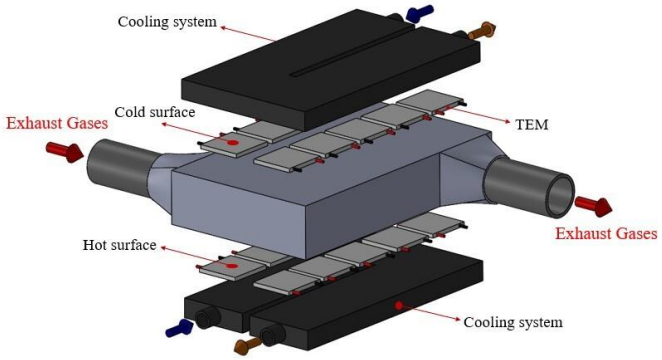

Fig. 2. TEG configuration.

C. Geometries

Since the heat transfer depends largely on the geometry of the exchanger used, three different geometries were proposed, as shown in Fig. 3.

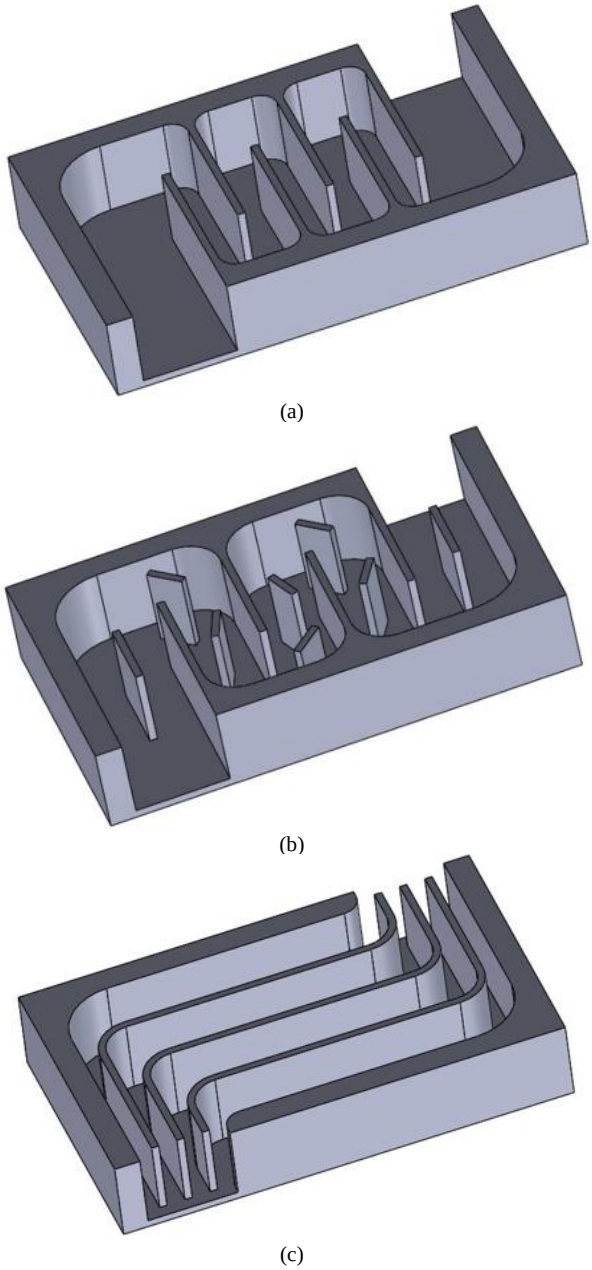

(a) (b) (c)

Fig. 3. Proposed geometries: (a) with snake path, (b) oblique fins, (c) with parallel paths.

The behavior of exhaust gases flowing through these exchangers was simulated using OpenFOAM® software. The geometry patterns correspond to snake paths (Fig. 3a), small oblique fins (Fig. 3b), and parallel paths (Fig. 3c). All of them were created in SolidWorks, and the meshing analysis was performed in the open-source software SALOME.

D. Boundary conditions

The single-cylinder diesel engine used in the experimental setup of the study is the SK-MDF300 model manufactured by SOKAN. This is a 4-stroke engine with a 20:1 compression ratio, which can generate a maximum power of 4.5 HP at 3600 rpm, while its injection system is direct with a 20 ° BTDC angle. The exchanger is modeled with copper material due to its good heat transfer properties. The heat flow at the inlet is 20 m/s

based on the operating characteristics of the engine. The internal walls of the heat exchanger are in contact with the exhaust gases flow while configured as standard walls. A convection heat transfer is established on the external walls, with a natural convection coefficient of $20\ W/m^2K$ and with an ambient temperature of 303.15 K.

E. Mesh quality control

A good mesh quality ensures better results for the CFD analysis as it minimizes the computational demand for the appropriate prediction of the phenomena. SALOME software, in which the meshing process was carried out, used the corresponding algorithm to calculate the defined geometric characteristics of the different elements that construct the mesh domain. There are different quality control criteria, including aspect ratio and skew. The first reveals the degree of conformity of a mesh element to the regular element of its type. The second reflects the angle between the lines that join opposite sides of a quadrangle element or the greatest angle between three medians in triangle elements [30]. The values obtained for these parameters are within the acceptable range defined by the software, as summarized in Table I.

TABLE I
FACE QUALITY CONTROLS

Geometry	Mesh metric	Min. value	Max. value
Snake path	Aspect ratio	1	1.6245
	Skew	0.0322	24.2985
Oblique fins	Aspect ratio	1	1.7826
	Skew	0.0083	35.4462
Parallel paths	Aspect ratio	1	1.6584
	Skew	0.0090	31.9546

F. Mesh independence analysis

The number of elements of a mesh determines how thin it is. Notice that the more number elements, the more accuracy is obtained within the calculations. However, more computing sources will be required. As a result, longer iteration times. Therefore, it is necessary to carry out a mesh independence analysis in order to determine the optimal point where stability in the calculations is reached. Fig 4 shows the temperature results obtained at a central point of each geometry by varying the number of elements of the tetrahedral mesh used.

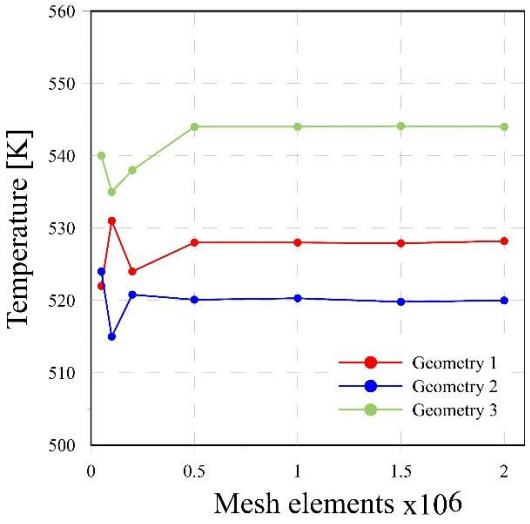

Fig. 4. Mesh Independence analysis for the geometries: (1) snake path, (2) oblique fins, (3) parallel paths (shown in Fig. 3).

The results show that the networks with 1,000,000 elements remained stable. At this point, the temperature readings do not fluctuate much, so they can be said to be reliable. This number of items is used to strike a balance between the reliability of the results and the computing resources used.

G. Experimental validation

In order to verify the reliability of the results of the simulations and take into account that the geometry shown in Fig. 5 is already built on a test bench in the engine laboratory at Universidad del Atlántico, this geometry was used to perform an experimental validation. To carry out this procedure, two test benches were used. The diesel test bench consists of a single-cylinder diesel engine, whose characteristics were detailed in section II D of this document, an alternator that allows controlling the engine's output power, and a data acquisition system (DAQ) by which engine parameters were controlled and measured. The second test bench was the TEG test bench, whose heat exchanger is shown in Fig. 5.

The TEG found in the test bench has 20 thermoelectric modules, type 12610-5.1, 10 located on the upper side of the heat exchanger, and 10 on the lower side (Fig. 6). These TEMs were composed of 126 Bismuth Telluride p–n junctions, each module has a size of 40 mm x 40 mm, and they could withstand temperatures up to 300 ºC for the hot side. From the temperature difference between the exhaust gases and a water current at 300.15 K, the TEM generates voltages whose value can be visualized through the instrumentation of the test bench.

The voltages generated by the 10 TEMs of the upper side will be the same or very similar to the voltages generated by the 10 TEMs of the lower side of the heat exchanger due to the symmetric geometry. Therefore, only the upper side of the heat exchanger will be analyzed.

On the other hand, through OpenFOAM®, the surface temperatures of the outer wall of the heat exchanger were obtained. Using these values and the TEMs characterization, which appears in the manufacturer's datasheet, it was possible to know the voltage values that the thermoelectric modules

would generate with the temperatures that the simulations showed.

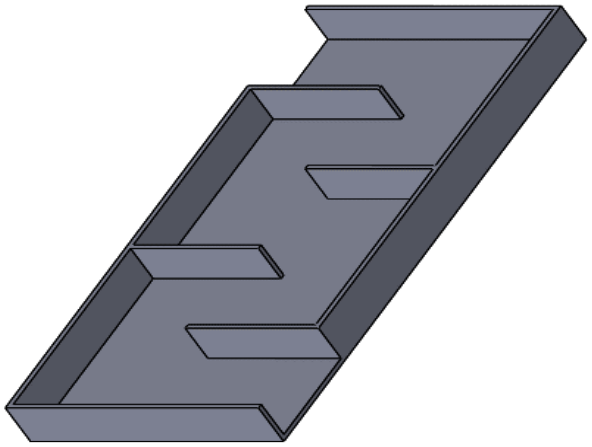

Fig. 5. Geometry used for experimental validation.

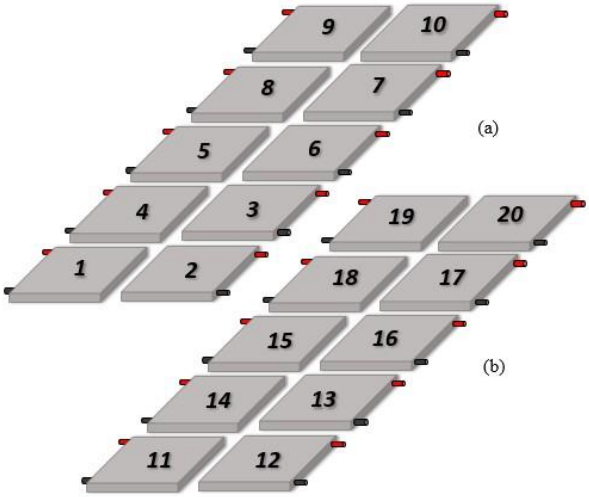

Fig. 6. TEM location in the heat exchanger of the test bench (a) upper side (b) lower side.

Fig. 7 shows a comparison between the results obtained experimentally (using the engine with 1800W load) and the results of the simulations. Based on the results, the curve described by both methodologies features similar behavior. Also, it can be verified in Table II that the average relative error between the two results is 2.23%, while the maximum and minimum errors are 5.6% and 1.06%, respectively. The difference between the results can be attributed to the uncertainty in the measurement instruments, small differences between the boundary conditions and the real conditions, simplifications made in the model, among others. Since the average relative error does not exceed 5%, it can be stated that the simulations performed are reliable. In this way, they provide a good approximation to reality.

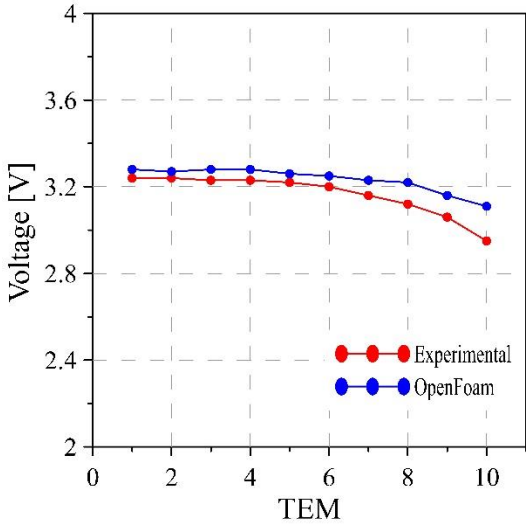

Fig. 7. Voltage results obtained experimentally and through OpenFOAM® software.

TABLE II
EXPERIMENTAL VALIDATION OF MEASURED AND SIMULATED VOLTAGE.

TEM	Voltage [V]		Error	
	Measured	Simulated	Absolute	Relative in %
1	3.24	3.28	0.04	1.32
2	3.24	3.27	0.03	1.06
3	3.23	3.28	0.05	1.39
4	3.23	3.28	0.05	1.42
5	3.22	3.26	0.04	1.38
6	3.2	3.25	0.05	1.69
7	3.16	3.23	0.07	2.06
8	3.12	3.22	0.10	3.09
9	3.06	3.16	0.10	3.35
10	2.95	3.11	0.16	5.58
			Average	**2.23**

III. RESULTS

After carrying out the simulations in OpenFOAM®, the Paraview software was used to visualize the results obtained with respect to each of the factors that influence energy recovery.

Fig. 8 shows the temperature profiles obtained for the upper and lower walls of the geometries. Each wall is in contact with 10 TEM, being 20 modules overall. It should be noted that, due to the symmetry of the figures, the temperature profile for the upper and lower faces will be practically the same.

Paraview allows observing the exact values of certain variables in specific points of the geometry. In this way, it was possible to estimate the surface temperature in 4 different points (Fig. 9) and compare the results obtained.

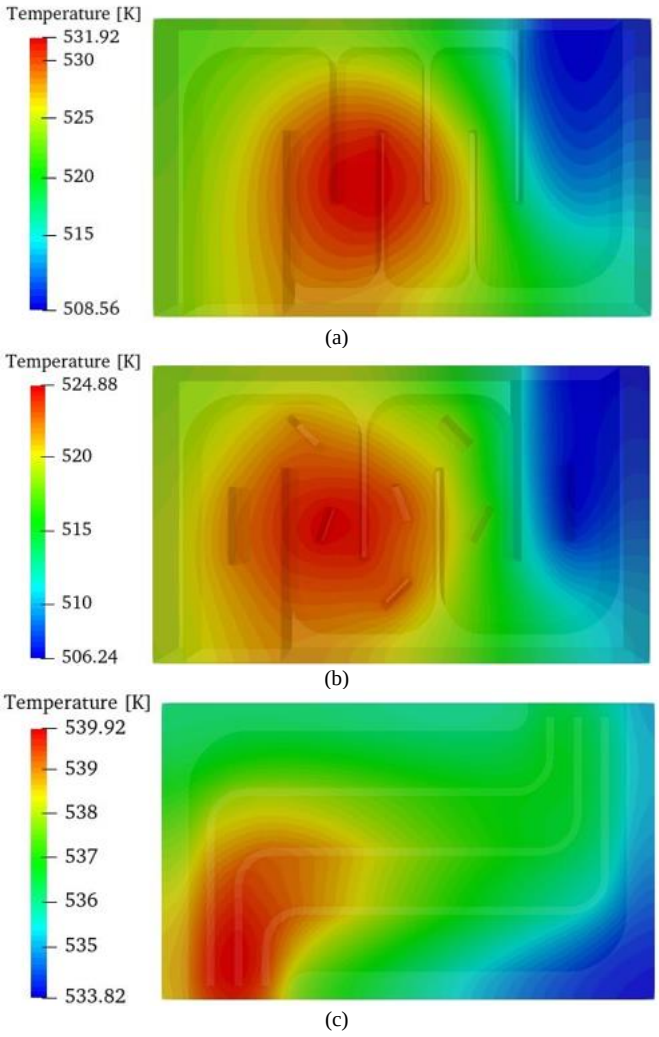

Fig. 8. Temperatures on the upper and lower outer walls of geometry: (a) with snake path, (b) oblique fins, (c) with parallel paths.

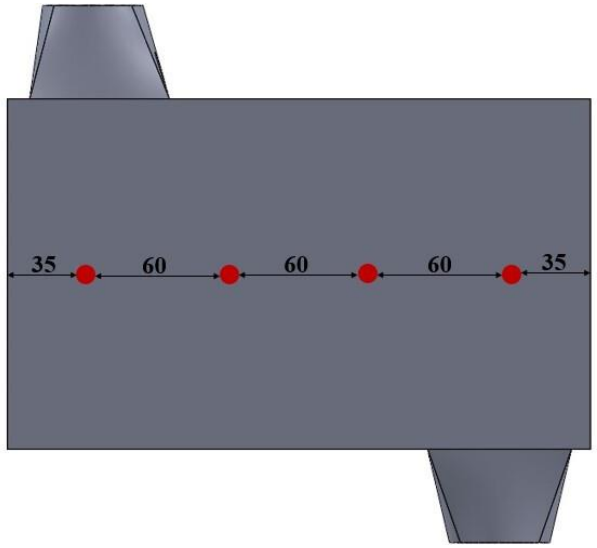

Fig. 9. Points chosen for the quantitative analysis of temperatures (distance in mm).

Fig. 10 shows the surface temperatures for the three geometries analyzed. It can be seen that the walls of the geometry with snake path reach temperatures of 511 K - 532 K, while the geometry with oblique fins reaches temperatures of 507 K - 525 K; on the other hand, the walls of geometry with parallel paths have temperatures between 531 K - 539 K, being this the geometry with the highest surface temperatures on its walls, which benefits the voltage and electric current generation.

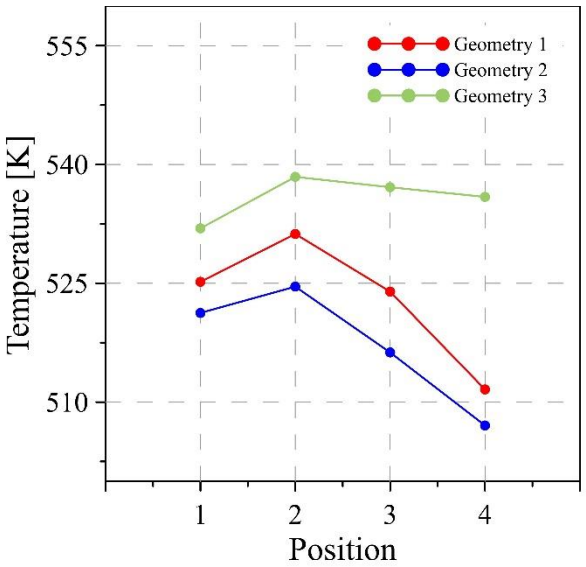

Fig. 10. Surface temperature of the external walls for the geometry with: (1) snake path, (2) oblique fins, (3) parallel paths.

Due to the temperature difference between the exhaust gases and the water-fed cooling system at 300.15 K, a wall heat flux occurs, whose values are shown in Fig. 11. As expected, the geometry with the best heat transfer is the third geometry (parallel paths), having a value of 3100 W/m^2.

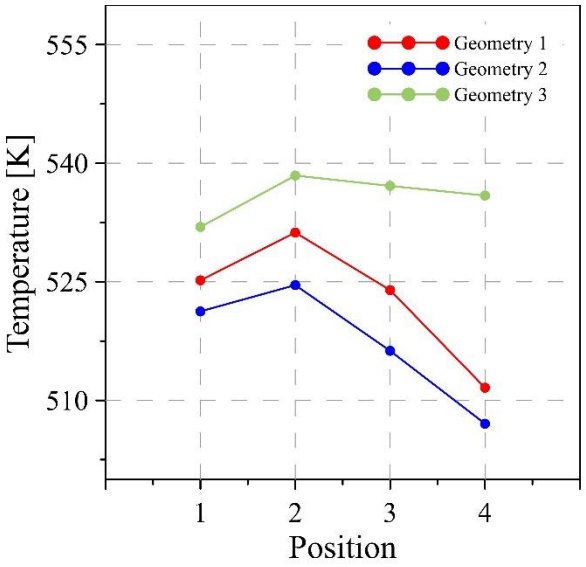

Fig. 10. Surface temperature of the external walls for the geometry with: (1) snake path, (2) oblique fins, (3) parallel paths.

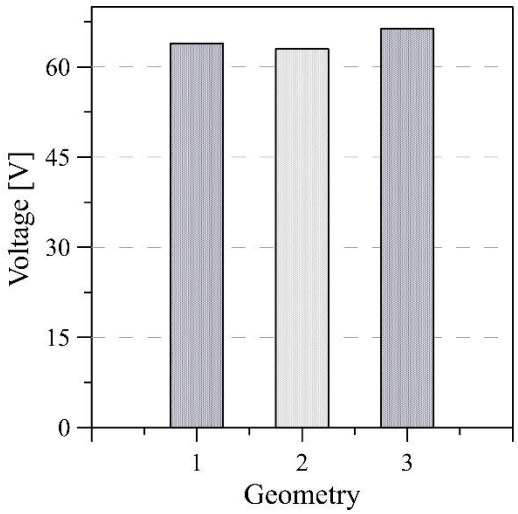

Fig. 12. Voltage generated by the TEMs using the geometry with: (1) snake path, (2) oblique fins, (3) parallel paths.

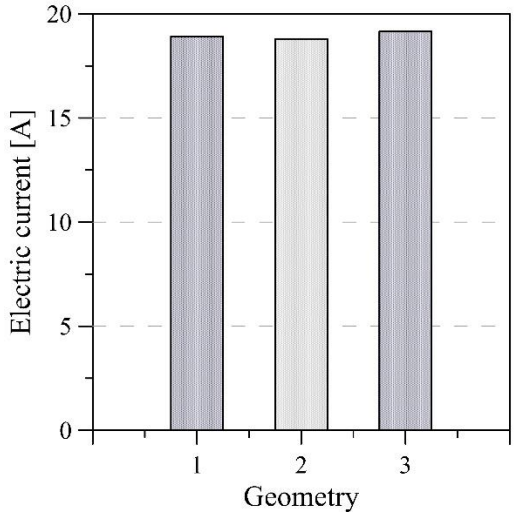

Fig. 13. Electric current generated by the TEMs using the geometry with: (1) snake path, (2) oblique fins, (3) parallel paths.

Once the temperature on each side of the modules is obtained and considering the information of the data sheet provided by the manufacturer, it was possible to calculate the total voltage and electric current that the TEMs would generate with the respective temperatures (Fig. 12 and 13). According to the results, the geometry with the highest values of surface temperature and heat transfer is also the one that generated the greatest voltage and electric current since the production of these two depends strictly on the temperature difference on each side of the module. However, the optimal geometry selection does not only depend on the voltage and electric current that can be generated but also on variables such as pressure, turbulence kinetic energy, and turbulence Eddy dissipation rate, since poor performance with regard to these factors can compromise the integrity of the engine under study.

As mentioned before, Paraview shows the exhaust gases pressure through the streamlines of the different heat exchanger geometries (Fig. 14); Thus, it was possible to calculate the total pressure drop of the fluid for each proposal. As shown in Fig. 15, the geometry that generates the greatest pressure drop is the one with a snake path (5010 Pa), while the geometry with a parallel path generates the least pressure drop (109 Pa). It should be noted that a high-pressure drop value indicates that the exhaust gases outlet pressure is being forced to reach the TEG outlet, so with respect to this factor, the geometry with the best performance is the one with a parallel path.

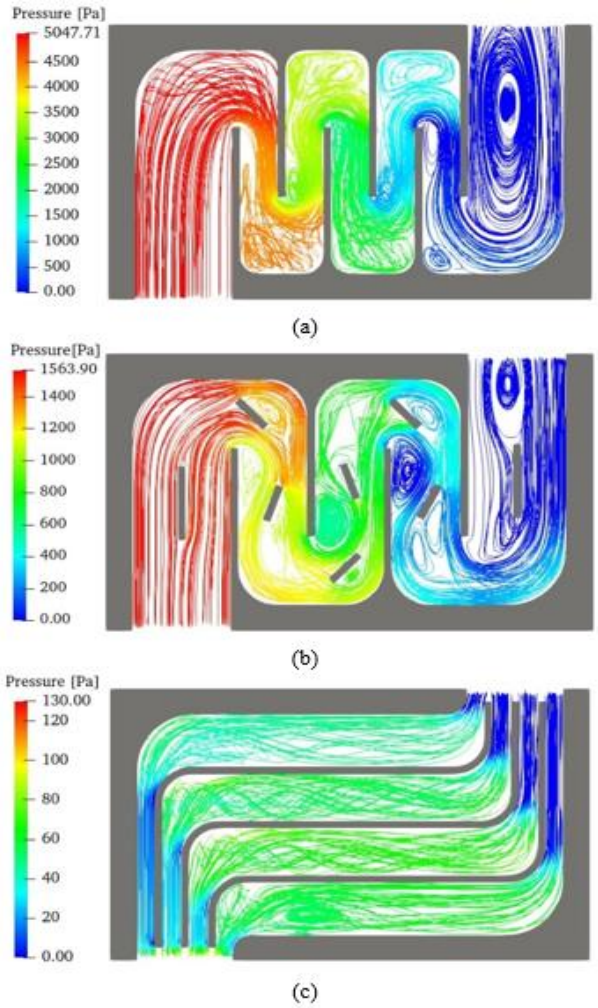

Fig. 14. Pressure profile for the geometry with: (a) snake path, (b) oblique fins, (c) parallel paths.

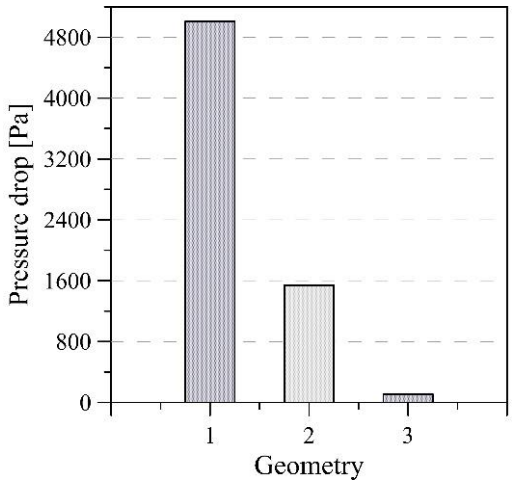

Fig. 15. Pressure drop in geometry with: (1) snake path, (2) oblique fins, (3) parallel paths.

On the other hand, the turbulence kinetic energy (TKE), associated with the presence of eddies, features the highest values in the geometry with a snake path, whereas the minimum is established in the geometry with the parallel path (Table III). This is related to the flow lines shown in the pressure profiles, where a greater presence of eddies is observed in Fig. 15a and Fig. 15 b.

Finally, Table III shows the values of the turbulence eddy dissipation rate for each of the geometries, indicating that the third geometry (parallel path) is the one with the best behavior with respect to this factor, having a TEDR of 346 m^2/s^3.

TABLE III
TURBULENCE KINETIC ENERGY AND EDDY DISSIPATION RATE OF THE GEOMETRIES UNDER STUDY

Geometry	Turbulence eddy dissipation rate $[m^2/s^3]$	Turbulence kinetic energy $[m^2/s^2]$
Snake path	51498	47.5
Oblique fins	9019	10.3
Parallel paths	346	1.4

The values shown in Table III, for both TEDR and TKE, demonstrate that the geometry with the best results with respect to these factors is the one with parallel paths since there is less presence of eddies, and it allows them to decrease more quickly than in other geometries. This behavior reduces the possibility of problems caused by emptiness or back pressures.

It is important to take these variables into account since if the chosen geometry would generate high voltages, but it would also have high TKE and TEDR values, its use would not be convenient since it could compromise the proper functioning of the engine to which the TEG is coupled.

CONCLUSIONS

By conducting this study, three different heat exchanger geometries (snake path, oblique fins, and parallel paths) were analyzed, with which energy recovery in a stationary single-cylinder diesel engine was analyzed. The OpenFOAM ® software was used to simulate the behavior of the exhaust gases when passing through each of the geometries, and using the ParaView tool, the results obtained could be observed.

Finally, it is concluded that the heat transfer achieved by the parallel path geometry was 3100 W/m^2, 21.57% and 27.05% higher than with the other geometries; while the voltage generated using geometries with snake path and oblique fins was 63.9 V and 62.9 V, the voltage generated using the one with the parallel path was 66.3 V, and the electric current was 19.15 A, so the values achieved by the TEMs using this geometry were also higher than those generated with the others. 65.55 W of power was recovered, and the conversion efficiency of 5.11% was reached using geometry with a parallel path. Other analyzed variables, such as pressure drop, TKE, and TEDR, also had their best values using the geometry with the parallel path. These were 109 Pa, 1.4 m^2/s^2 and 346 m^2/s^3, respectively. In accordance with the above, it can be affirmed that geometry with a parallel path not only benefits the generation of voltage and electric current but also ensures the proper operation of the engine under study.

It should be noted that the geometry with parallel paths was the one with the best results among the proposed geometries. However, more rigorous optimization studies can be carried out in which variables such as wall thickness, rounding radius, among others, are analyzed in order to get even better results.

Finally, it is important to remember that the implementation of a CFD simulation software in the optimization analysis of the heat exchanger coupled to the TEG represents an option to realize a device that exhibits an adequate behavior with respect to each of the factors influencing the energy recovery, without spending money and raw materials by implementing various failed options until you reach the correct one.

REFERENCES

[1] J. Yu and H. Zhao, "A numerical model for thermoelectric generator with the parallel-plate heat exchanger," *J. Power Sources*, vol. 172, no. 1, pp. 428–434, 2007, doi: 10.1016/j.jpowsour.2007.07.045.

[2] C. Alberto, R. Piedrahita, R. A. Acosta, Y. Alberto, and C. Sánchez, "The combustion engine as a mechatronic object in mechanical technology undergraduate curriculum," *Sci. Tech.*, vol. 18, no. 1, pp. 95–100, 2013, doi: 10.22517/23447214.8717.

[3] M. Hatami, D. D. Ganji, and M. Gorji-Bandpy, "A review of different heat exchangers designs for increasing the diesel exhaust waste heat recovery," *Renew. Sustain. Energy Rev.*, vol. 37, pp. 168–181, 2014, doi: 10.1016/j.rser.2014.05.004.

[4] R. Ramírez, A. S. Gutiérrez, J. J. Cabello Eras, K. Valencia, B. Hernández, and J. Duarte Forero, "Evaluation of the energy recovery potential of thermoelectric generators in diesel engines," *J. Clean. Prod.*, vol. 241, 2019, doi: 10.1016/j.jclepro.2019.118412.

[5] L. E. Hombach, L. Doré, K. Heidgen, H. Maas, T. J. Wallington, and G. Walther, "Economic and environmental assessment of current (2015) and future (2030) use of E-fuels in light-duty vehicles in Germany," *J. Clean. Prod.*, vol. 207, pp. 153–162, 2019, doi: 10.1016/j.jclepro.2018.09.261.

[6] A. Cardona Vargas, J. Jaramillo Álvarez, and A. Amell Arrieta, "Mechanical and environmental performance evaluation of a Spark Ignition Engine with high compression ratio fueled whit Biogas, Methane and Hydrogen blends," *Sci. Tech.*, vol. 25, no. 01, pp. 65–76, 2020.

[7] E. A. Salazar Marin, J. F. Arroyave Londoño, and B. Guevara Rojas, "Desarrollo de un vehículo solar híbrido 'XUE revolution,'" *Sci. Tech.*, vol. 21, no. 4, p. 297, 2016, doi: 10.22517/23447214.12831.

[8] E. A. Salazar Marín, J. F. Arroyave Londoño, and I. Y. Moreno Ortiz, "Analysis of performance of a converted electric vehicle," *Sci. Tech.*, vol. 25, no. 1, pp. 37–44, 2020, doi: 10.22517/23447214.21231.

[9] A. E. Teo Sheng Jye, A. Pesiridis, and S. Rajoo, "Effects of mechanical turbo compounding on a turbocharged diesel engine," *SAE Tech. Pap.*, vol. 1, 2013, doi: 10.4271/2013-01-0103.

[10] A. T. Hoang, "Waste heat recovery from diesel engines based on Organic Rankine Cycle," *Appl. Energy*, vol. 231, no. September, pp. 138–166, 2018, doi: 10.1016/j.apenergy.2018.09.022.

[11] S. N. Hossain and S. Bari, "Waste heat recovery from the exhaust of a diesel generator using Rankine Cycle," *Energy Convers. Manag.*, vol. 75, pp. 141–151, 2013, doi: 10.1016/j.enconman.2013.06.009.

[12] H. Koppauer, W. Kemmetmüller, and A. Kugi, "Modeling and optimal steady-state operating points of an ORC waste heat recovery system for diesel engines," *Appl. Energy*, vol. 206, no. September, pp. 329–345, 2017, doi: 10.1016/j.apenergy.2017.08.151.

[13] N. M. Sakhare, P. S. Shelke, and S. Lahane, "Experimental Investigation of Effect of Exhaust Gas Recirculation and Cottonseed B20 Biodiesel Fuel on Diesel Engine," *Procedia Technol.*, vol. 25, no. Raerest, pp. 869–876, 2016, doi: 10.1016/j.protcy.2016.08.195.

[14] P. Divekar, Q. Tan, X. Chen, and M. Zheng, "Characterization of Exhaust Gas Recirculation for diesel low temperature combustion," *IFAC-PapersOnLine*, vol. 28, no. 15, pp. 45–51, 2015, doi: 10.1016/j.ifacol.2015.10.007.

[15] M. Zheng, G. T. Reader, and J. G. Hawley, "Diesel engine exhaust gas recirculation - A review on advanced and novel concepts," *Energy Convers. Manag.*, vol. 45, no. 6, pp. 883–900, 2004, doi:

10.1016/S0196-8904(03)00194-8.
[16] M. He, E. Wang, Y. Zhang, W. Zhang, F. Zhang, and C. Zhao, "Performance analysis of a multilayer thermoelectric generator for exhaust heat recovery of a heavy-duty diesel engine," *Appl. Energy*, vol. 274, no. May, p. 115298, 2020, doi: 10.1016/j.apenergy.2020.115298.
[17] D. Champier, "Thermoelectric generators: A review of applications," *Energy Convers. Manag.*, vol. 140, pp. 167–181, 2017, doi: 10.1016/j.enconman.2017.02.070.
[18] I. Temizer and C. Ilkiliç, "The performance and analysis of the thermoelectric generator system used in diesel engines," *Renew. Sustain. Energy Rev.*, vol. 63, pp. 141–151, 2016, doi: 10.1016/j.rser.2016.04.068.
[19] S. Vale, L. Heber, P. J. Coelho, and C. M. Silva, "Parametric study of a thermoelectric generator system for exhaust gas energy recovery in diesel road freight transportation," *Energy Convers. Manag.*, vol. 133, pp. 167–177, 2017, doi: 10.1016/j.enconman.2016.11.064.
[20] P. Fernández-Yañez, O. Armas, A. Capetillo, and S. Martínez-Martínez, "Thermal analysis of a thermoelectric generator for light-duty diesel engines," *Appl. Energy*, vol. 226, no. May, pp. 690–702, 2018, doi: 10.1016/j.apenergy.2018.05.114.
[21] E. S. Mohamed, "Development and performance analysis of a TEG system using exhaust recovery for a light diesel vehicle with assessment of fuel economy and emissions," *Appl. Therm. Eng.*, vol. 147, no. January 2018, pp. 661–674, 2019, doi: 10.1016/j.applthermaleng.2018.10.100.
[22] B. Orr, A. Akbarzadeh, M. Mochizuki, and R. Singh, "A review of car waste heat recovery systems utilising thermoelectric generators and heat pipes," *Appl. Therm. Eng.*, vol. 101, pp. 490–495, 2016, doi: 10.1016/j.applthermaleng.2015.10.081.
[23] C. Q. Su, W. S. Wang, X. Liu, and Y. D. Deng, "Simulation and experimental study on thermal optimization of the heat exchanger for automotive exhaust-based thermoelectric generators," *Case Stud. Therm. Eng.*, vol. 4, pp. 85–91, 2014, doi: 10.1016/j.csite.2014.06.002.
[24] M. M. Aslam Bhutta, N. Hayat, M. H. Bashir, A. R. Khan, K. N. Ahmad, and S. Khan, "CFD applications in various heat exchangers design: A review," *Appl. Therm. Eng.*, vol. 32, no. 1, pp. 1–12, 2012, doi: 10.1016/j.applthermaleng.2011.09.001.
[25] W. H. Chen, Y. X. Lin, Y. Bin Chiou, Y. L. Lin, and X. D. Wang, "A computational fluid dynamics (CFD) approach of thermoelectric generator (TEG) for power generation," *Appl. Therm. Eng.*, vol. 173, no. February, p. 115203, 2020, doi: 10.1016/j.applthermaleng.2020.115203.
[26] E. Pavan Kumar, A. Kumar Solanki, and M. Mohan Jagadeesh Kumar, "Numerical investigation of heat transfer and pressure drop characteristics in the micro-fin helically coiled tubes," *Appl. Therm. Eng.*, vol. 182, no. September 2020, p. 116093, 2021, doi: 10.1016/j.applthermaleng.2020.116093.
[27] W. C. Lin, Y. M. Ferng, and C. C. Chieng, "Numerical computations on flow and heat transfer characteristics of a helically coiled heat exchanger using different turbulence models," *Nucl. Eng. Des.*, vol. 263, pp. 77–86, 2013, doi: 10.1016/j.nucengdes.2013.03.051.
[28] "OpenFOAM Features," 2019. https://cfd.direct/openfoam/features/.
[29] S. B. Pope, *Turbulent Flows*. 2013.
[30] "SALOME Platform documentation: Mesh User's," 2016. https://docs.salome-platform.org/7/gui/SMESH/index.html.

Evelyn Peñafiel Guzmán. Barranquilla native, Mechanical engineer at Universidad del Atlántico, located in Barranquilla, Colombia in 2021.

ORCID: https://orcid.org/0000-0001-5136-2085

Osmar Bermúdez Turizo. Barranquilla native, Mechanical engineer at Universidad del Atlántico, located in Barranquilla, Colombia in 2021.

ORCID: https://orcid.org/0000-0003-4979-8896

Jorge Duarte Forero. Barranquilla native, Colombia. He is an associated professor of the Mechanical Engineering Program at Universidad del Atlántico. He received his BSME from Universidad del Atlántico, located in Barranquilla, Colombia in 2007. Master in Mechanical Engineering from Universidad del Norte, Barranquilla, Colombia in 2013. Ph. D in Engineering from Universidad del Norte, Colombia in 2017. He is a MINCIENCIAS – Senior Researcher.
ORCID: http://orcid.org/0000-0001-7345-9590